CHAPTER 3. CONVERGENCE ANALYSIS

This chapter contains an analysis of the convergence of the CRLS-SA algorithm. The analysis is based on the concept of convergence time constant [17], [85], which is defined as the ratio of the sensitivity and the condition number.

3.1. Condition Number

The condition number is defined as:

$$c\left(\hat{\mathbf{R}}\right)=\frac{l_{\max}\left(\hat{\mathbf{R}}\right)}{l_{\min}\left(\hat{\mathbf{R}}\right)} \tag{3.1.1}$$

where $l_{\max}\left(\hat{\mathbf{R}}\right)$ and $l_{\min}\left(\hat{\mathbf{R}}\right)$ are the maximum and minimum eigenvalues of the *NxN* sample auto-correlation matrix $\hat{\mathbf{R}}$, of a wss vector signal $\boldsymbol{y}_n$ of size *N*, defined on the basis of

$$\hat{r}_k=\frac{1}{N}\sum_{n=0}^{N-1-k} y_n\, y_{n-k}\;; \qquad k=0,1,\ldots,N-1 \tag{3.1.2a}$$

where

$$\boldsymbol{y}_n=[y_n\; y_{n-1}\cdots y_{n-N+1}] \tag{3.1.2b}$$

$$\hat{\mathbf{R}}=\begin{bmatrix} r_0 & \cdots & r_{N-1} \\ \vdots & \ddots & \vdots \\ r_{N-1} & \cdots & r_0 \end{bmatrix} \tag{3.1.3}$$

Given that $S(w)$ is the power spectral density of y_n, the condition number is bounded by [32]:

$$c\left(\hat{\mathbf{R}}\right)=\frac{l_{\max}\left(\hat{\mathbf{R}}\right)}{l_{\min}\left(\hat{\mathbf{R}}\right)}\le\frac{\max_w S(w)}{\min_w S(w)} \tag{3.1.4}$$

For an AR process of order *N*, the components of $\boldsymbol{y}_n$ are generated by:

$$y_n = \frac{1}{1 - A(z)} x_n \tag{3.1.5}$$

where $A(z) = \sum_{i=1}^{N} a_i z^{-i}$ and x_n is white Gaussian noise. The power spectral density (PSD) of the AR process y_n can be written in terms of $S_i(w)$, the PSD for a pole pair (complex conjugates):

$$S(w) = \prod_{i=1}^{N} S_i(w) \tag{3.1.6}$$

Because of interactions among the poles, the peaks of the PSD due to each pole pair can be different from the peaks of the PSD for that pole pair itself without interaction, i.e. for a second order AR process. Let:

$$w_{i,\max} = \arg\max_{w} S_i(w) \tag{3.1.7a}$$

and

$$w_{i,\min} = \arg\min_{w} S_i(w) \tag{3.1.7b}$$

so that we have for any w_i (and therefore in particular for $w_{i,\max}$ or $w_{i,\min}$)

$$S(w_{i,\max}) \underset{b}{\overset{a}{\gtrless}} S_i(w_{i,\max}) \Leftrightarrow \prod_{\substack{k=1 \\ k \neq i}}^{N} S_k(w_{i,\max}) \underset{b}{\overset{a}{\gtrless}} 1 \tag{3.1.8}$$

Under condition a, $\forall i$, it follows that

$$\begin{aligned} \max_{w} S(w) &\geq \max_{k} S(w_{k,\max}) \\ &\geq S_k(w_{k,\max}); k = 1, \cdots, N \end{aligned} \tag{3.1.9}$$

Equations (3.1.9) tend to be satisfied analytically, as supported experimentally, when the poles of the AR process are closely spaced, and say that the biggest peak of $S(w)$ exceeds the largest PSD peak for any individual constituent pole pair. Figure 3.1.1 shows the condition of

(3.1.9). Using analogous reasoning, condition *b* leads to the minimum of $S(w)$ being smaller than the minimum of any individual pole pair PSD, that is

$$\min_{w} S(w) \le S_k(w_{k,\min}); k = 1, \cdots, N \tag{3.1.10}$$

Condition (3.1.10) is also shown in Figure 3.1.1. Figure 3.1.2 shows the PSD for individual poles and the combined poles when the poles are spaced far apart. We see in Figure 3.1.2 that the peak of the PSD for the combined poles is smaller the highest peak of the PSD for the individual poles.

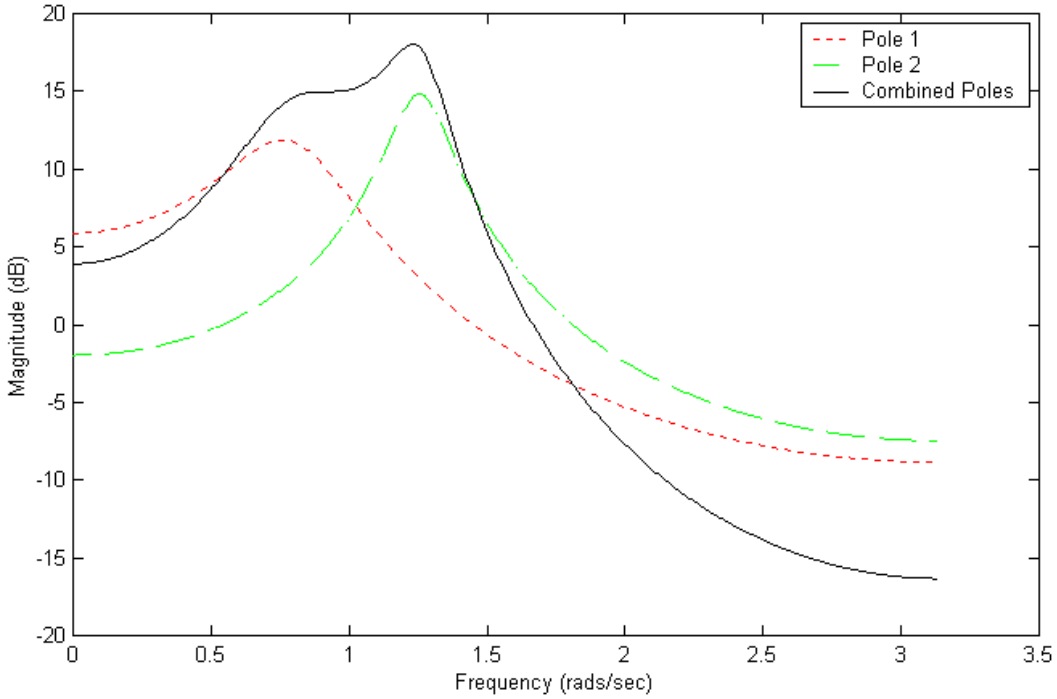

Figure 3.1.1 Spectrum of Closely-Spaced AR Process.

For a direct form AR (DFAR) process with tightly clustered poles, condition *a* in (3.1.8) is likely to hold for $w_{i,\max}$ resulting in (3.1.9) for $\max_{w} S(w)$, while condition *b* is likely to hold for $w_{i,\min}$ resulting in (3.1.10) for $\min_{w} S(w)$. Hence we surmise from using (3.1.4) that for an

order *N* DFAR process with tightly clustered poles, the condition number is always greater than the condition number for any of its constituent individual second order AR processes.

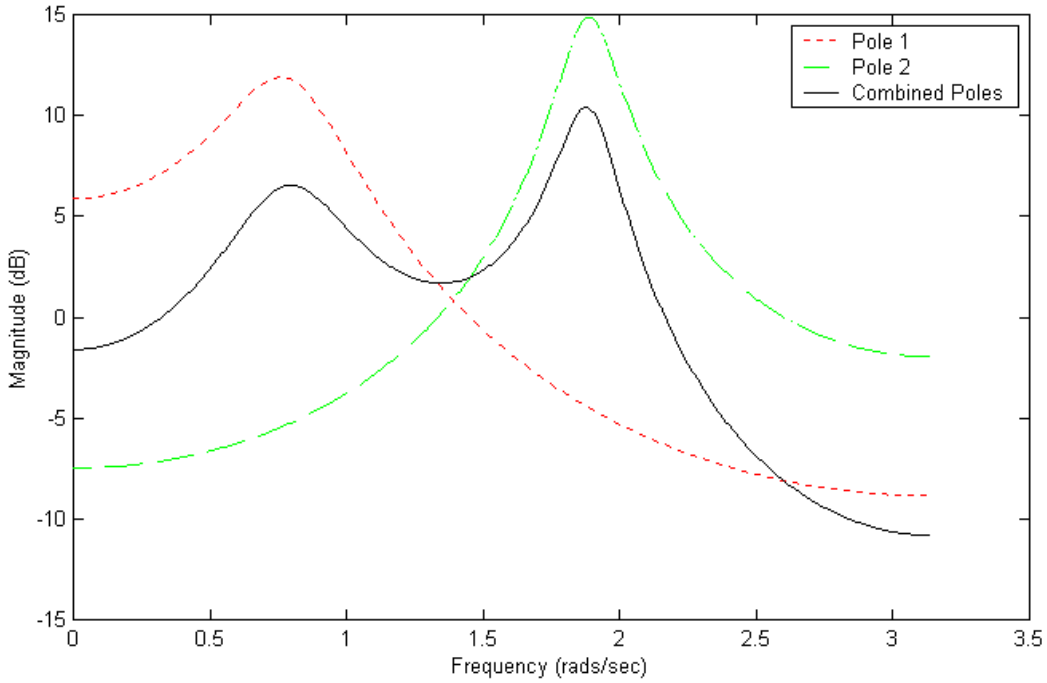

Figure 3.1.2 Spectrum of Well-Separated AR Process.

We offer two cases as examples:

- Case I - a fourth order AR process with poles that are tightly clustered, and
- Case II - a fourth order AR process with poles that are well separated.

The theoretical results for the condition number are shown in Table 3.1.1. Note that the poles in Case I and Case II have the same pole radii. The only difference is that the poles for Case I are closely spaced while the poles for Case II are far apart.

Table 3.1.1 Condition Number

Case	Pole 1	Pole 2	DF	Section 1	Section 2
Case I	$.8e^{\pm jp/8}$	$.9e^{\pm jp/5}$	1950	12.3	5.7
Case II	$.8e^{\pm jp/8}$	$-.9e^{\pm jp/5}$	3.9	1.5	5.7

For a higher order AR prediction error filter (PEF) in cascade form, the input signal to the *i*-th section of the cascade structure can be expressed as

$$y_{n,i} = \frac{\prod_{k=1}^{i-1}\left(1-\hat{A}_k(z)\right)}{1-A(z)}x_n \tag{3.1.11}$$

where $\hat{A}_k(z)$ is the estimate for the *k*-th section. The input to the first cascade PEF section, $y_{n,1}$, is equal to y_n. This shows that the input signal to the first section reflects all of the poles, just as for the input signal to the DFAR parameter estimator, while the input signal to the last section tends to reflect only poles that have not been (approximately) removed by the previous sections. Hence, the auto-correlation matrix of the input signal to the first cascade PEF section is the same as a 2*x*2 diagonal component of the *NxN* auto-correlation matrix $\hat{\mathbf{R}}$ of the DF. Note that each 2x2 diagonal block represents the auto-correlation of a conjugate pole pair (a section). As a result, the maximum eigenvalue of the first section of the cascade is always less than the maximum eigenvalue of the DF and the minimum eigenvalue of the first section of the cascade is always bigger than the minimum eigenvalue of the DF. In other words, the condition number of the first section of the cascade is always less than the condition number of the DF. This can be explained as follows. Let [75]

$$l_1 \le l_2 \le \ldots \le l_n$$

be the eigenvalues of a Hermitian matrix $A \in R^{nxn}$, and

$$\mu_1 \le \mu_2 \le \ldots \le \mu_{n-1}$$

be the eigenvalues of a matrix $B \in R^{n-1 x n-1}$, where B is a principal submatrix of A, then

$$\lambda_1 \le \mu_1 \le \lambda_2 \le \mu_2 \le \ldots \le \lambda_{n-1} \le \mu_{n-1} \le \lambda_n$$

For the final section in the cascade, if (3.1.9) and (3.1.10) hold, the condition number is smaller than that for the DF. For any other sections, (3.1.9) and (3.1.10) hold if the poles are closely spaced. In other words, the condition number of each section of the cascade structure is always smaller than the condition number of the DF for signals with closely spaced poles, such as speech signals for example.

3.2. Sensitivity

Sensitivity can be defined [17][3] as:

$$\begin{aligned} S &= \sum_{i=1}^{N} S_i \\ S_i &= \sum_{n=0}^{\infty} \left| \frac{\partial h(n,q)}{\partial q_i} \right|^2 \end{aligned} \tag{3.2.1}$$

where $h(n,q)$ is the impulse response, q are the parameters in the structure, and N is the number of coefficients. Define the impulse response of the DF PEF for an AR process with N coefficients as:

$$h_n^{DF} = [1 - \hat{A}(z)]d_n \tag{3.2.2}$$

where

$$\hat{A}(z) = \sum_{i=1}^{N} \hat{a}_i z^{-i} \tag{3.2.3}$$

Now the derivative of the impulse response with respect to each coefficient is

$$\begin{aligned}\frac{\partial h_n^{DF}}{\partial a_i} &= \frac{\partial\left(1-\hat{A}(z)\right)}{\partial a_i} d_n \\ &= -z^{-i} d_n \\ &= -d_{n-i}\end{aligned} \tag{3.2.4}$$

where d_n is the unit sample sequence. By substituting (3.2.4) into (3.2.1), the sensitivity of a DF PEF with respect to its coefficients is:

$$S_i^{DF} = \left|-d_{n-i}\right|^2 = 1 \tag{3.2.5a}$$

and the total sensitivity of the DF is

$$\begin{aligned}S^{DF} &= \sum_{i=1}^{N} S_i^{DF} \\ &= N\end{aligned} \tag{3.2.5b}$$

The system response of a cascade structure PEF, with each section a second order filter, is

$$1-\hat{A}(z) = \prod_{i=1}^{M}\left(1-\hat{A}_i(z)\right) \tag{3.2.6a}$$

$$\hat{A}_i(z) = \sum_{l=1}^{2} \hat{a}_{i,l} z^{-l} \tag{3.2.6b}$$

where *M=N/2*, and its impulse response is

$$h_n^C = \left(\prod_{i=1}^{M} 1-\hat{A}_i(z)\right) d_n \tag{3.2.7}$$

We can show that the derivative of the impulse response with respect to each coefficient is

$$\begin{aligned}\frac{\partial h_n^C}{\partial a_{k,l}} &= -z^{-l}\left(\prod_{\substack{i=1\\ i\neq k}}^{M} 1-\hat{A}_i(z)\right) d_n \\ &= -z^{-l}\,\frac{1}{1-\hat{A}_k(z)}\left(\prod_{i=1}^{M} 1-\hat{A}_i(z)\right) d_n \\ &= -\frac{z^{-l}}{1-\hat{A}_k(z)}\; h_n^C\end{aligned} \tag{3.2.8}$$

where l=1,2. The sensitivity of the cascade structure can be obtained by using (3.2.8) in (3.2.1), resulting in:

$$\begin{aligned}S^C &= \sum_{i=1}^{N} S_i^C \\ S_i^C &= \sum_{n=0}^{\infty}\left|-\frac{z^{-l}}{1-\hat{A}_k(z)}\; h_n^C\right|^2\end{aligned} \tag{3.2.9}$$

From (3.2.8) we see that the derivative of the impulse response of the cascade structure with respect to the coefficients of the *k-th* section is obtained by delaying the impulse response of all sections but the *k-th* section. We also see that the derivative of the impulse response of the *k-th* section (or the sensitivity of the coefficients of the *k*-th section) can be obtained by filtering the delayed final impulse response with $\frac{1}{1-\hat{A}_k(z)}$, similar to the gradient computation indicated in Section 2.3. Here we see, by comparing (3.2.5b) and (3.2.9), that the DF has potentially low sensitivity compared to the cascade structure. Note that for the DF PEF, a change in a coefficient will affect all its roots, being the zeros in this case. On the other hand, changing a coefficient in a section of the cascade structure will affect only the roots of that section.

Using the pole structure for Case I and II, as given in Section 3.1, the sensitivities of the DF and cascade structure PEFs are computed. The theoretical results are shown in Table 3.2.1.

Table 3.2.1 Sensitivity

Case	Pole 1	Pole 2	DF	Section 1	Section 2
Case I	$.8e^{\pm jp/8}$	$.9e^{\pm jp/5}$	4.0	6.5	7.1
Case II	$.8e^{\pm jp/8}$	$-.9e^{\pm jp/5}$	4.0	6.5	7.1

We see that the DF PEF has a lower sensitivity than the cascade structure PEF. Note that for section 2, Case I and II yield the same sensitivity because the poles are the same. For section 2, the radii of the poles for Case I and II are the same, but the corresponding peak frequency is different. As a result of (3.2.9), and because the radii of their poles are the same, the sensitivities for Case I and II are also the same. We can prove this as follows. Denote the polynomials for the second pole pairs in Case I and Case II respectively as:

$$A_{I,q2}(z) = 1 - 2r\cos q_2\, z^{-1} + r^2 z^{-2} \tag{3.2.10a}$$

$$\begin{aligned} A_{II,q2}(z) &= 1 - 2r\cos(p - q_2) z^{-1} + r^2 z^{-2} \\ &= 1 + 2r\cos q_2\, z^{-1} + r^2 z^{-2} \end{aligned} \tag{3.2.10b}$$

The total impulse responses for Case I and Case II are then:

$$\begin{aligned} h_I &= A_{I,q1} A_{I,q2}\, d_n \\ &= A_{I,q1}\left(d_n - 2r\cos q_2\, d_{n-1} + r^2 d_{n-2}\right) \end{aligned} \tag{3.2.10c}$$

$$\begin{aligned} h_{II} &= A_{II,q1} A_{II,q2}\, d_n \\ &= A_{II,q1}\left(d_n + 2r\cos q_2\, d_{n-1} + r^2 d_{n-2}\right) \end{aligned} \tag{3.2.10d}$$

where $A_{I,q1}$ and $A_{II,q1}$ are the same. The derivatives of the impulse response for Case I with respect to the coefficients of the second section are:

$$\frac{\partial h_I}{\partial r} = A_{I,q1}\left(-2\cos q_2\, d_{n-1} + 2r\, d_{n-2}\right) \tag{3.2.10e}$$

$$\frac{\partial h_I}{\partial \cos q_2} = A_{I,q1}\left(-2rd_{n-1}\right) \tag{3.2.10f}$$

The derivatives of the impulse response for Case II with respect to the coefficients of the second section are:

$$\frac{\partial h_{II}}{\partial r} = A_{II,q1}\left(+2\cos q_2\, d_{n-1} + 2r\ d_{n-2}\right) \tag{3.2.10g}$$

$$\frac{\partial h_{II}}{\partial \cos q_2} = A_{II,q1}\left(+2rd_{n-1}\right) \tag{3.2.10h}$$

From (3.2.10e)-(3.2.10h) we see that the derivative of the impulse response, with respect to the coefficients of the second section, are - except for the sign - the same for Case I and Case II. Hence, by using (3.2.1), we see that $A_{I,q2}$ and $A_{II,q2}$ have the same sensitivities.

Even though the DF has a lower sensitivity than the cascade structure, this does not mean that the overall effect on the system of a change in the DF parameters is less than the overall effect of a parameter change in the cascade structure. To verify this, a small perturbation is imposed on the parameters of the DF and cascade structures. Then the distances between the true system and the perturbed DF and cascade structures are compared. The Itakura distance is used, as it is considered more appropriate than the Euclidean distance for measuring the distance between two sets of highly correlated linear prediction filters (LP) [19]. The Itakura distance is defined as:

$$d\left[A(z), B(z)\right] = \log\frac{\boldsymbol{b}^T\mathbf{R}\boldsymbol{b}}{\boldsymbol{a}^T\mathbf{R}\boldsymbol{a}} \tag{3.2.11a}$$

where $\mathbf{R}$ is as defined in (3.1.3), but of size $(N+1)x(N+1)$, and the LP prediction parameter polynomials to be compared are:

$$A(z) = \sum_{i=1}^{N} a_i z^{-i} \tag{3.2.11b}$$

$$B(z) = \sum_{k=1}^{N} b_k z^{-k} \tag{3.2.11c}$$

$$\boldsymbol{a} = [a_1 \; a_2 \cdots a_N \;]^T \tag{3.2.11d}$$

$$\boldsymbol{b} = [b_1 \; b_2 \cdots b_N \;]^T \tag{3.2.11e}$$

Averaging over 100 realizations we found that for closely spaced poles (Case I), the Itakura distance of the DF PEF is 17.59 after perturbing its parameters, while for the cascade structure PEF it is 1.81. For poles that are spaced far apart (Case II), the Itakura distance of the DF PEF is 1.18 after parameter perturbation, while for the cascade structure PEF it is 1.81. For these simulations, the coefficients were perturbed by adding a small random quantity (zero mean, equal variance of .001). We also see here that sensitivity alone does not characterize the structure. In the Case I and Case II DF systems above, which exhibit the same sensitivity, the effect of parameter perturbation is quite different. On the other hand, for the corresponding cascade systems, the parameter perturbations yield the same Itakura distance.

3.3. Convergence Time Constant

Define the convergence time constant t [17] for the direct form as:

$$t = \frac{condition\ number}{sensitivity} \tag{3.3.1}$$

and for the cascade structure use

$$t_c = \prod_{k=1}^{M} t_k \tag{3.3.2}$$

where t_k is the convergence time constant for the *k-th* section, and *M=N/2* with *N* being the order of the filter.

To substantiate the conjectured behaviors, some simulations are conducted. Using the condition number result from Section 3.1 and the sensitivity result from Section 3.2, the convergence parameters for poles that are closely spaced are shown in Table 3.3.1 (which also includes results for Case II).

Table 3.3.1 Convergence Time Constant

Case			DF	Section 1	Section 2	Section 1+2
	Pole 1	Pole 2				
Case I	$.8e^{\pm jp/8}$	$.9e^{\pm jp/5}$	487	1.87	.8	1.4
Case II	$.8e^{\pm jp/8}$	$-.9e^{\pm jp/5}$	.975	.22	.8	.16

Using (3.1.1) for the condition number and (3.2.5b) and (3.2.9) for the DF and cascade sensitivity respectively, we see in Table 3.3.1 that for an AR process with poles that are tightly clustered, as in Case I, the cascade structure will have a smaller convergence time constant than the DF. Hence the cascade structure is expected to converge faster than the DF. For a higher order AR process with poles that are well separated, there is a possibility that the DF will converge as fast as, or maybe faster than, the cascade structure does. In other words, for a system with poles that are far apart, some sections of the cascade structure might converge faster than the DF, while other sections might converge more slowly.

It is difficult to determine the convergence rate from the trajectory of the coefficients. Instead, we measure the Itakura distance between the estimated and the true denominator polynomial at any time instant *n*. Then we look at how fast these distances, for the DF and cascade structures, reach steady state and how small the distance has become.

Some simulation experiments are conducted to get an idea of the performance of CRLS-SA. First, we simulate the two fourth order AR processes that generate Case I and Case II signals. The first system has poles that are closely spaced as given for Case I. We see in Figure 3.3.1 that CRLS-SA converges much faster than DF in terms of Itakura distance. This corresponds to the convergence time constant t for CRLS-SA, which at 1.4 is much smaller than that for DF, which is 487 (see Table 3.3.1 Case 1). From the trajectory of the coefficients in Figure 3.3.2, it is difficult to see the convergence rate difference between CRLS-SA and DF.

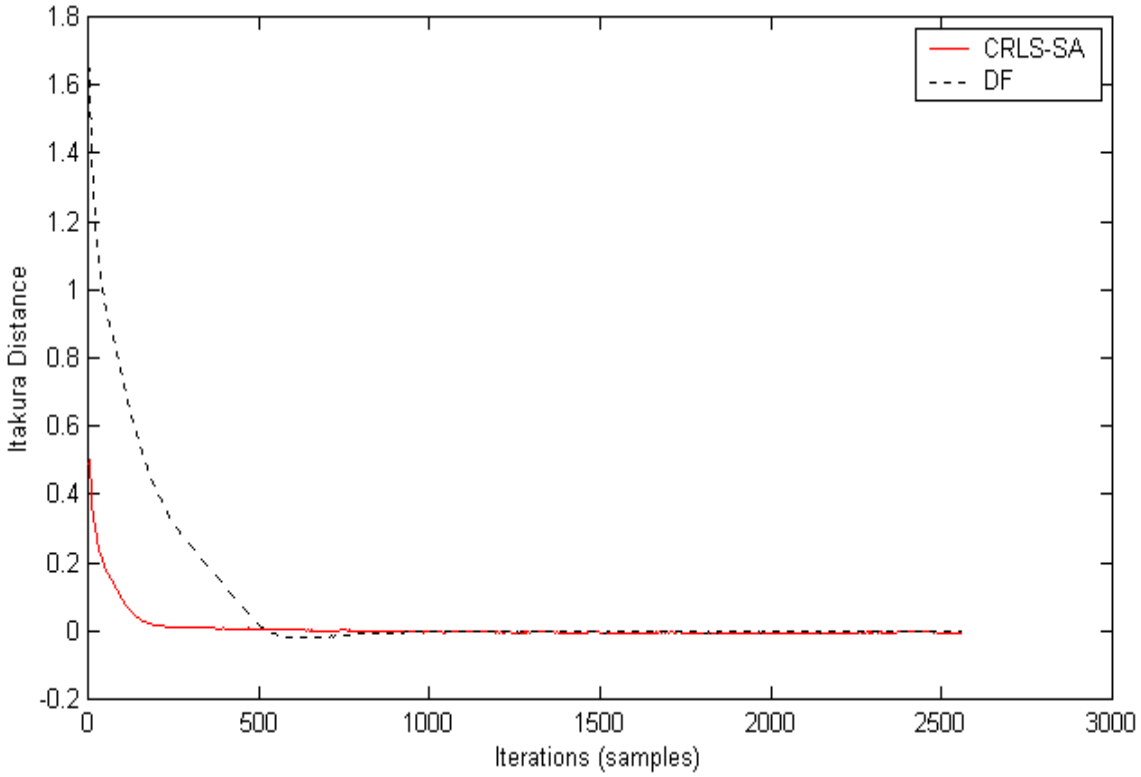

Figure 3.3.1 Itakura Distance for CRLS-SA and DF for Case I.

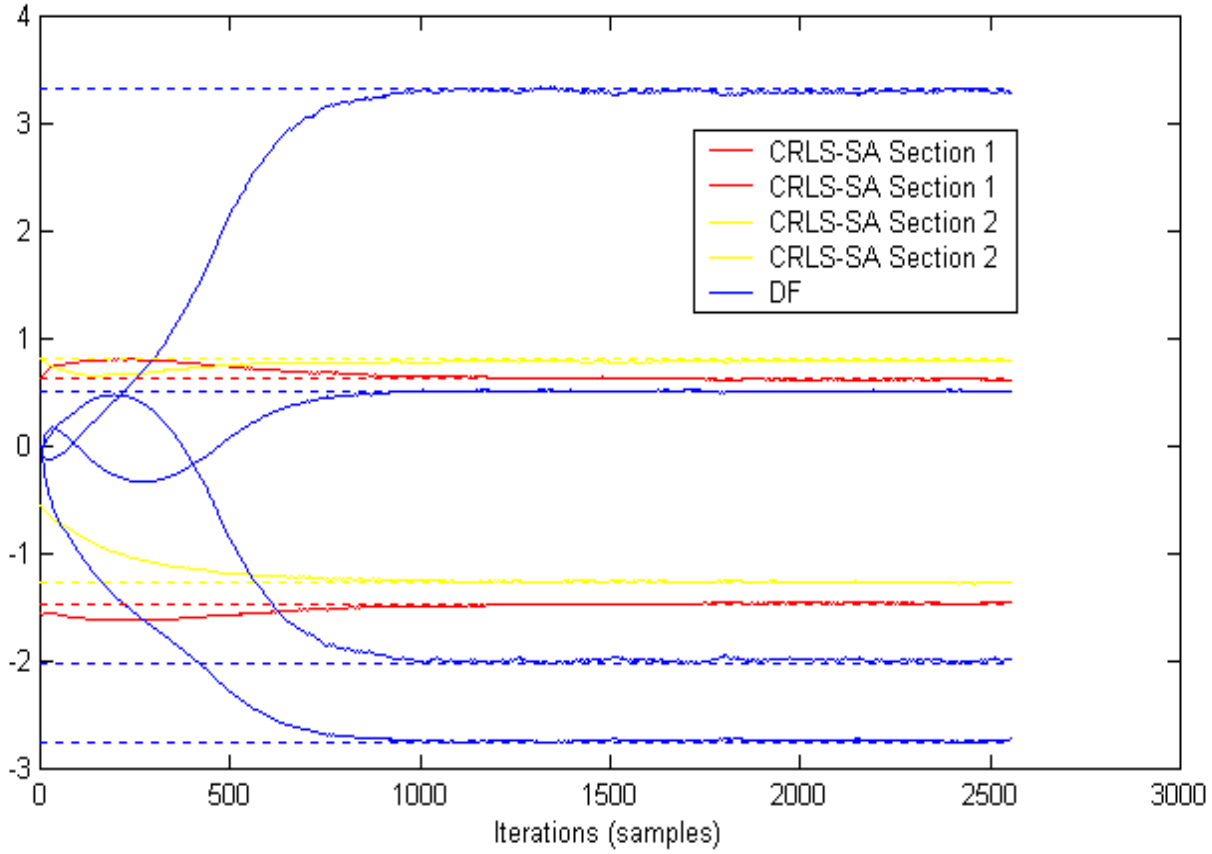

Figure 3.3.2 Coefficient Trajectories for CRLS-SA and DF for Case I.

The second system has poles that are far apart (Case II). Now we see in Figure 3.3.3 that CRLS-SA converges just a little bit faster than DF. This corresponds to the convergence time constant for CRLS-SA, shown in Figure 3.3.4, being just a little bit smaller than for the DF (see also Table 3.3.1 Case II). In Figure 3.3.5, we see the coefficient trajectories for CRLS-SA and DF. Again, it is difficult to determine the convergence rate from the coefficient trajectories.

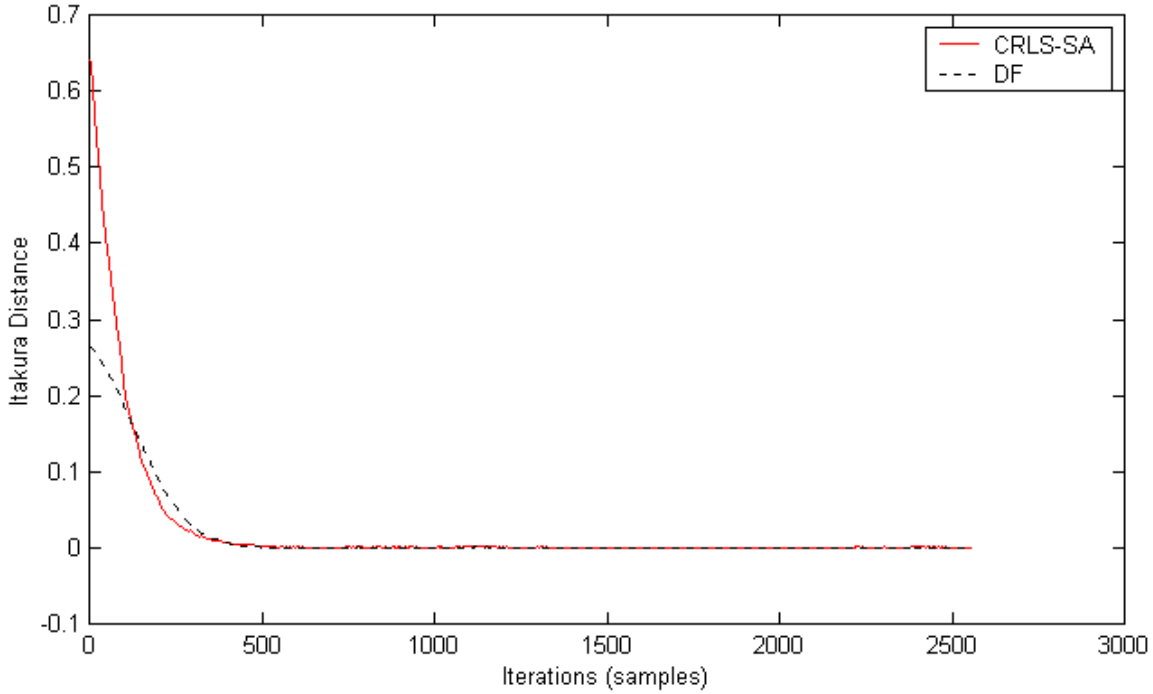

Figure 3.3.3 Itakura Distance for CRLS-SA and DF for Case II.

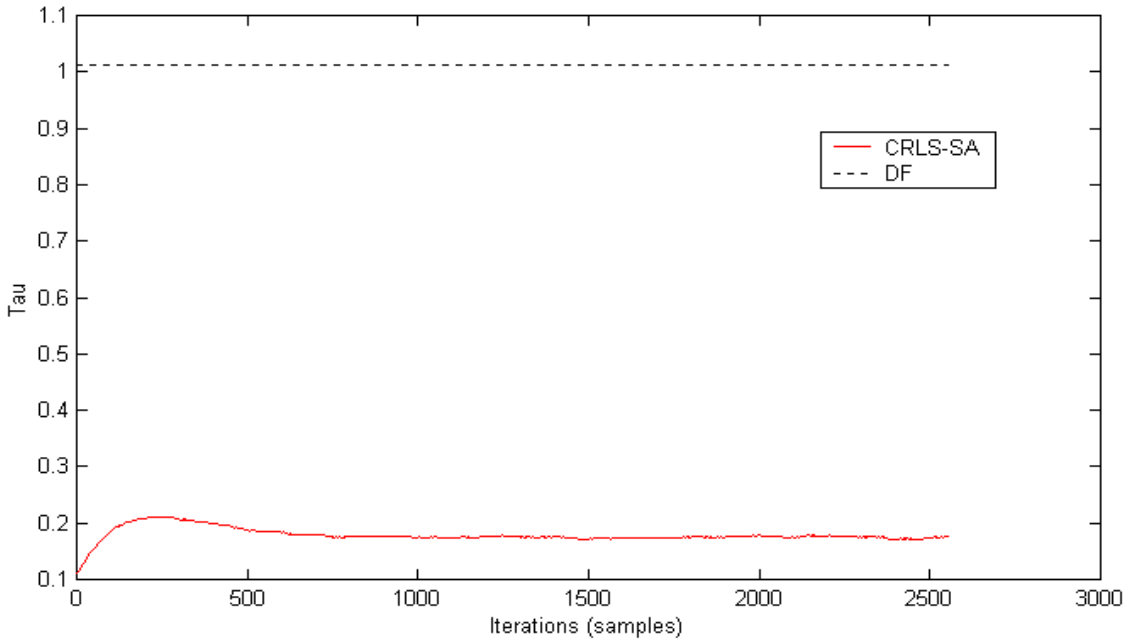

Figure 3.3.4 Convergence Time Constant for CRLS-SA and DF for Case II.

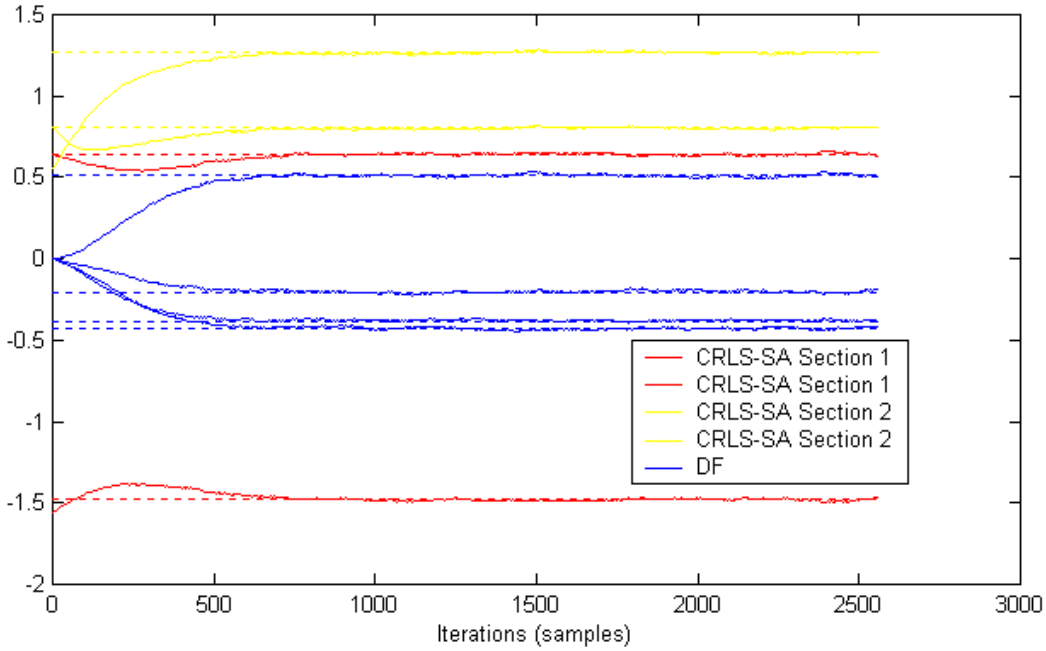

Figure 3.3.5 Coefficient Trajectories for CRLS-SA and DF for Case II.

The next simulation example uses 10^{th} order AR processes. The coefficients of the AR processes are obtained from speech signals. That is, from a frame of speech, we estimate the AR coefficients. Then we use these estimates to generate outputs for the corresponding AR process. The original speech frames were chosen to correspond to voiced and unvoiced speech respectively. Note that voiced speech is a segment of speech that shows periodicity, while the unvoiced speech is a segment of speech that does not show any periodicity. Also, the spectrum of voiced speech usually shows dominant spectral content in the low frequency range, as shown in Figure 3.3.6, while unvoiced speech shows either dominant spectral content in the high frequency range or a flat spectrum (see Figure 3.3.7).

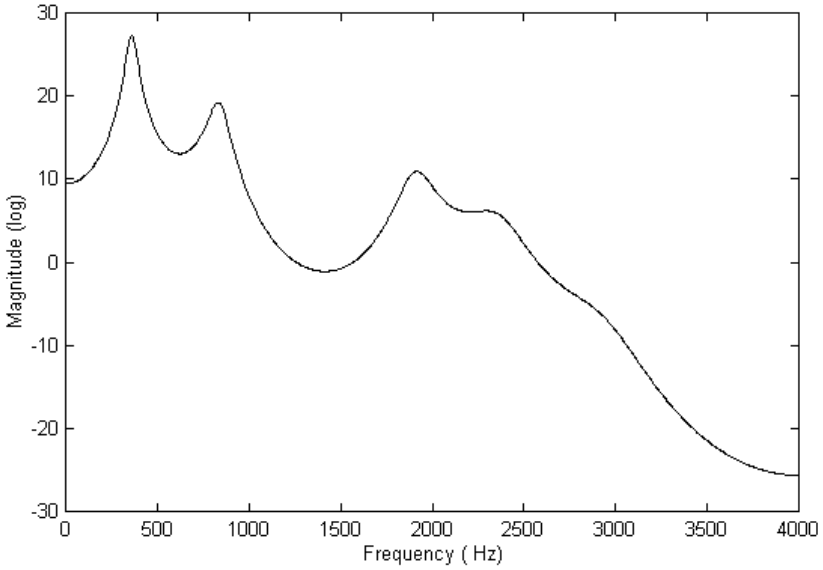

Figure 3.3.6 Spectrum of Voiced Speech Realization.

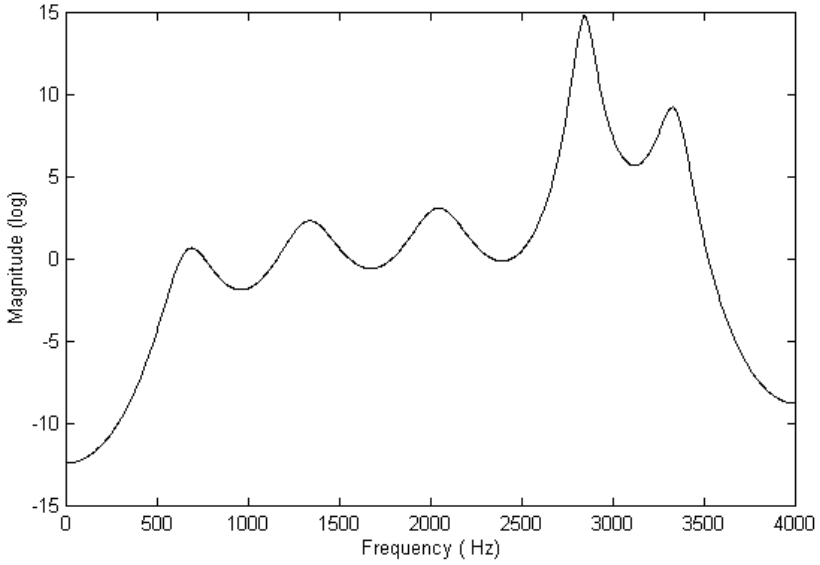

Figure 3.3.7 Spectrum of Unvoiced Speech Realization.

The results for CRLS-SA, along with those for DF, are shown in Figures 3.3.8 and 3.3.9 for voiced and unvoiced speech frames respectively. We see from Figure 3.3.8 that, as the

conjecture suggests, for a convergence time constant (of about 0.3) for CRLS-SA, which is much smaller than that for DF (of about 124), the Itakura distance for CRLS-SA reaches steady state faster than for DF. We see the CRLS-SA converges at almost the same time for voiced and unvoiced speech. This means that CRLS-SA approaches the true system faster than DF. For the unvoiced speech in Figure 3.3.9, we see that, as the conjecture suggests, for a convergence time constant (of about 1.5) for DF which is just a little bit larger than that (of about 0.04) for CRLS-SA, DF converges just a little bit slower than CRLS-SA.

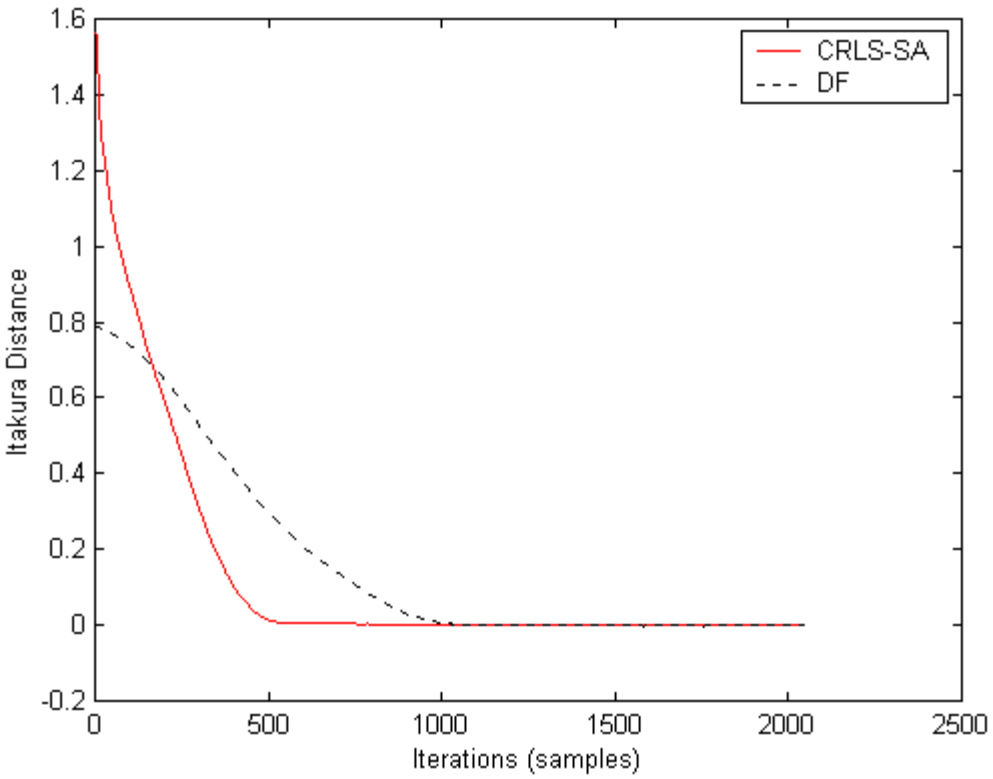

Figure 3.3.8 Itakura Distance for CRLS-SA and DF - Voiced Speech.

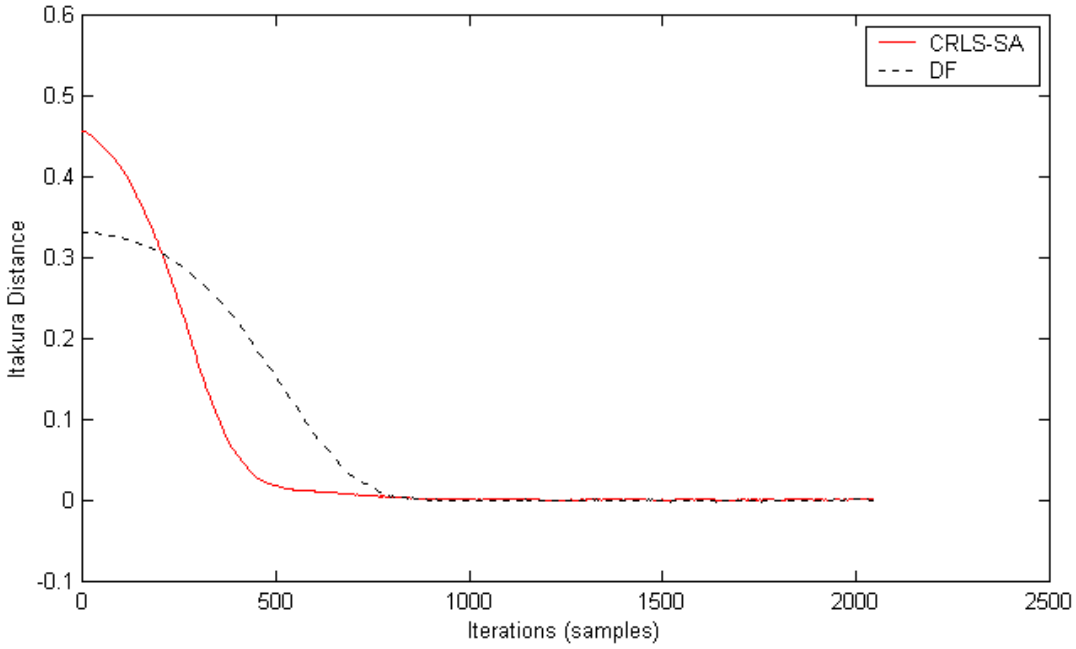

Figure 3.3.9 Itakura Distance for CRLS-SA and DF - Unvoiced Speech.

In the literature a cascade adaptive filter has been proposed, where each section is adapted locally, i.e. a cascade structure with successive adaptation [65]. In this scheme, each section is optimized based entirely on the parameters and signals in that section, and there is no attempt at finding the global minimum. The problem with this scheme is that it will be difficult to do estimation for closely spaced poles, i.e. a high order system, because from the point of view of each section, it is like an underdetermined estimation problem.

For comparison, we show in Figures 3.3.10 and 3.3.11 that the cascade with successive adaptation (CSA), i.e. local adaptation, does not provide good estimates compared to CRLS-SA, as shown by the fact that its Itakura distance is larger than that for CRLS-SA, and also by the fact that it reaches steady state very slowly. Note that for a fair comparison, the CSA is also adapted using the RLS algorithm. In Figure 3.3.10 we see that the CSA shows some inclination to converge at first, but it then stays at a higher Itakura distance compared to CRLS-SA. This is

because the CSA seems able to estimate the dominant poles but is not able to correctly estimate the other weaker poles since it does not try to find the global minimum. Moreover, since for a high order AR process, i.e. 10^{th} order in this case, the poles can not be far apart, CSA exhibits convergence difficulties. The convergence result of CSA for voiced speech in Figure 3.3.10 looks better than the convergence result of CSA for unvoiced speech in Figure 3.3.11. This can be explained by the fact that for unvoiced speech the poles usually exhibit almost equally strong resonance, see Figure 3.3.7, and as a result the CSA scheme has difficulty estimating the competing poles.

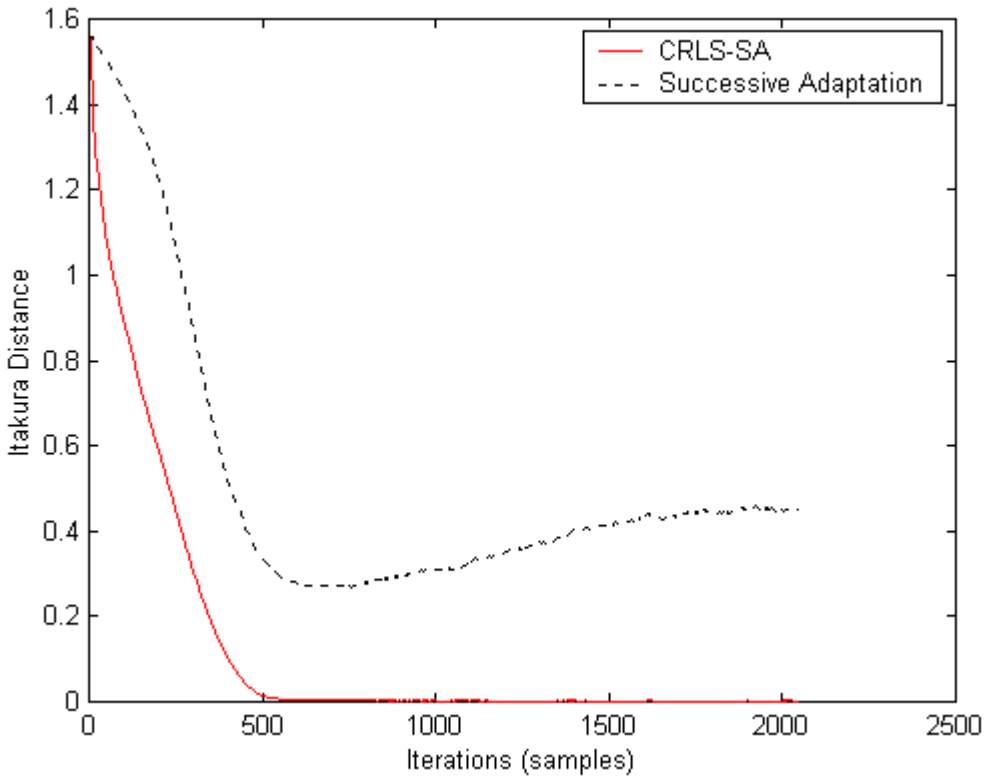

Figure 3.3.10 Itakura Distance for CRLS-SA and CSA - Voiced Speech.

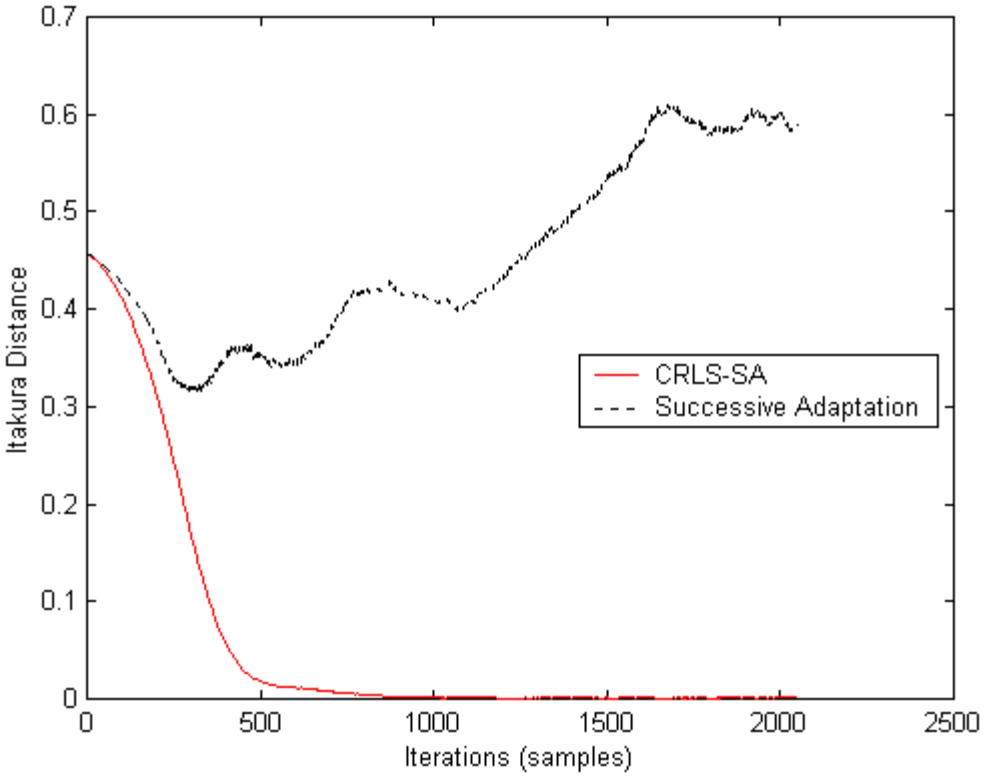

Figure 3.3.11 Itakura Distance for CRLS-SA and CSA - Unvoiced Speech.

We can now draw some conclusions. CRLS-SA converges faster than DF for linear prediction applications, especially for systems where the poles are tightly clustered. This is as predicted by the convergence time constant conjecture, because the convergence time constant for CRLS-SA is smaller than that for DF. The condition number of each section of the CRLS-SA structure is pretty much determined by its own pole pair, as there is little influence from the poles of the other sections, unlike as is the case with the DF. For a real system in which the order is relatively high, the pole locations cannot be very far apart, so that interaction among the poles can not be avoided. This makes CRLS-SA a more favorable choice than DF for real systems, such as used in speech processing.

The sensitivity by itself is not a perfect tool to characterize a system. A small change in a DF parameter produces a small change in its sensitivity, but it produces a large change in the overall system, especially for systems that have tightly clustered poles. A small change in the parameters of a section in the cascade form can produce a larger change in its sensitivity, however this does not usually correspond to a large change in the overall system. This is because a change in a section of the cascade structure will affect only that section, while the other sections remain intact. The conjectured convergence time constant, which is the ratio of the condition number and the sensitivity, predicts the relative convergence rate of the CRLS-SA and DF structures well.

The Itakura distance shows how close the estimated system is to the true system. Even though the individual estimated coefficients may not appear to be close to the true parameters, the Itakura distance shows that the overall system is actually quite close.